

# THE BARBADOS CLOUD OBSERVATORY ANCHORING INVESTIGATIONS OF CLOUDS AND CIRCULATION ON THE EDGE OF THE ITCZ

BY BJORN STEVENS, DAVID FARRELL, LUTZ HIRSCH, FRIEDHELM JANSEN, LOUISE NUIJENS, ILYA SERIKOV, BJÖRN BRÜGMANN, MARVIN FORDE, HOLGER LINNE, KATRIN LONITZ, AND JOSEPH M. PROSPERO

This document is a supplement to “The Barbados Cloud Observatory Anchoring Investigations of Clouds and Circulation on the Edge of the ITCZ,” by Bjorn Stevens, David Farrell, Lutz Hirsch, Friedhelm Jansen, Louise Nuijens, Ilya Serikov, Björn Brüggmann, Marvin Forde, Holger Linne, Katrin Lonitz, and Joseph M. Prospero (*Bull. Amer. Meteor. Soc.*, **97**, 787–801) • ©2016 American Meteorological Society • *Corresponding author*: Bjorn Stevens, Max-Planck-Institut für Meteorologie, Bundesstrasse 53, 20146 Hamburg, Germany • E-mail: [bjorn.stevens@mpimet.mpg.de](mailto:bjorn.stevens@mpimet.mpg.de) • DOI:10.1175/BAMS-D-14-00247.2

## GROUND-BASED INSTRUMENTATION.

The core Barbados Cloud Observatory (BCO) instruments consist of a multichannel multiwavelength Raman lidar system, a Ka-band cloud radar, a Ka-band Micro Rain Radar, a ceilometer, an all-sky imager, and a standard weather sensor. These instruments are described further below.

*Raman lidar.* The lidar uses a pulsed lidar beam and measures the elastic scattered light, the pure rotational Raman spectra (PRRS), and the rotational–vibrational Raman spectra of atmospheric molecules. Isolating individual spectral features of the atmospheric response, we apply the Raman lidar technique to characterize the scattering properties of atmospheric aerosols and to measure the air temperature and humidity. The lidar measures at nine spectral channels up to altitudes of 15 km, with a 7.5-m range gate. Three telescopes permit near-, mid-, and far-field measurements. The different products that can be obtained from the lidar are

particle backscatter, particle extinction, depolarization ratio, lidar ratio, water vapor mixing ratio, aerosol optical depth, and temperature. The present Raman lidar system measures water vapor mixing ratio and humidity during nighttime hours only, providing every other measurement round the clock during rain-free conditions. A new higher-powered system, which will allow daytime humidity measurements, is being developed and is scheduled to become operational in early 2017. The combination of particle backscatter measured at three wavelengths, particle extinction measured at two wavelengths, and particle depolarization ratio will also give information on the aerosol types. Particle backscatter is derived directly as the ratio of atmospheric lidar returns in the elastic to the pure rotational Raman channels. Thanks to the relatively small difference in the wavelength of backscattered light for these two channels, the corresponding differential atmospheric extinction is negligible. More information about the individual measurements is provided in Table ES1.

**TABLE ESI. Quantities derived from Raman lidar system.**

Physical quantity	Measurement principle
Particle backscatter	Measured at 355, 532, and 1,064 nm with Klett algorithm implemented for the retrieval in the infrared and calculated through a ratio of elastic and pure rotational Raman signals in ultraviolet and visible spectral range.
Particle extinction	Derived directly from atmospheric attenuation of pure rotational Raman signals at 355 and 532 nm.
Depolarization ratio	Measured at 532 nm as a ratio of two components of lidar backscatter signal having their vectors of the electromagnetic field oriented perpendicular and parallel with respect to those of the linearly polarized sounding laser beam.
Water vapor mixing ratio	Derived as a ratio of rotational–vibrational Raman signals due to water vapor and nitrogen molecules with excitation at 355 nm.
Air temperature	Measured at 355 nm with a pure rotational Raman lidar technique.

**Scanning cloud radar.** The radar is a scanning Ka-band (35.5 GHz) polarized Doppler cloud radar with a high sensitivity ( $-52$  dBZ at 5 km with 100-m range gates and 30-s averaging). Usually the radar is operated with 30-m range gates and 10-s averages (e.g., Lonitz et al. 2015). At 35 GHz, one expects attenuation in the presence of water vapor and condensate but much less than in the W band. As such, this frequency range strikes a good compromise between achieving the sensitivity that one desires for sensing clouds and the range required to profile through the depth of the atmosphere. The radar was named KATRIN, for Katrin Lehmann, a brilliant young scientist who died in a hiking accident in May 2009, shortly before she was to have joined the BCO team. KATRIN's antenna can be scanned with a full  $360^\circ$  in azimuth and  $\pm 90^\circ$  in elevation. The 1.2-m antenna has a beamwidth of  $0.5^\circ$ . The radar reaches full sensitivity at a range of 500 m and hence provides a good cloud-base detection capability. The high-range resolution of up to 10 m (typically 30 m) together with the narrow beamwidth allows for finescale observations of the cloud structure. The Doppler velocity resolution of up to  $0.05 \text{ m s}^{-1}$  provides insight into the turbulent fine structure of clouds. The radar receives the linear polarized signal in co- and cross-polarized orientation and thus provides the linear depolarization ratio (LDR) that is very helpful information to discriminate between different target types, such as liquid from ice, or insects. The system is fully automated and remotely controlled.

For roughly the first year of operation, KATRIN alternated between azimuth scans [first at four elevation angles ( $5^\circ$ ,  $12^\circ$ ,  $22^\circ$ , and  $45^\circ$ ) and later only at the lower two elevations], range–height indicator scans, and vertical staring. The scanning data were used to evaluate whether there was an apparent island effect by comparing joint height versus reflectivity

histograms at different ranges and at different times of the day, but a significant signal was not found and thereafter (since 20 December 2011) the radar has only been operated in a vertically pointing mode. The vertically pointing mode is preferred for a number of reasons: an analysis of the scanning data showed that the radar range (which is limited to about 15 km by attenuation when scanning at low elevation angles) was not sufficient to measure convective life cycles, the vertically pointing mode is advantageous for microphysical retrievals, and not scanning entails less wear and tear on the instrumentation.

**Micro Rain Radar.** The Micro Rain Radar (MRR-2) is a frequency-modulated continuous-wave radar operating in the K band (24 GHz). It retrieves the drop size distributions and its moments, radar reflectivity, and fall velocity of hydrometeors simultaneously on vertical profiles extending up to 3 km. As such, it can sample the entire rain system from shallow convective systems whose tops are frequently below 3 km. Two MRRs are deployed on Barbados: one at the BCO and one at the Caribbean Institute for Meteorology and Hydrology (CIMH). Both instruments are configured to have a vertical resolution of 100 m so as to provide sufficient range coverage. Because of the high sensitivity and fine temporal resolution, very small amounts of precipitation (below the threshold of conventional rain gauges) can be detected. For the chosen configuration, the manufacturer specifies a detection threshold of  $0.01 \text{ mm h}^{-1}$  at 500 m for an averaging time of 10 s. The large scattering volume (compared to in situ sensors) allows us to derive statistically stable drop size distributions within a few seconds. The droplet number concentration in each drop diameter bin is derived from the backscatter intensity in each corresponding frequency bin. In this procedure, an

empirical relation between terminal fall velocity and drop size is exploited.

**Ceilometer.** A Jenoptik 15k laser ceilometer with a 0.4-mrad field of view measures backscattered energy at 1,064-nm wavelength. The ceilometer is designed to operate up to heights of 15 km with a spatial resolution of 15 m and a temporal resolution of 30 s, although individual returns are increasingly difficult to distinguish from background noise with increasing altitude, limiting its effectiveness at the highest rate of sampling to the lower 4 km of the atmosphere. Nuijens et al. (2014) demonstrated that the ceilometer returns are useful to derive cloud-base heights (which include actual cloud-base heights but also cloud edges) by comparing gradients in returns to a threshold based on the background noise level. During the period between 6 December 2011 and 9 March 2012, the 15k model has been temporarily replaced by the Jenoptik 15k-X model. The 15k-X has a larger, 1.7-mrad field of view and is thus subject to more background noise during daylight hours, especially at low zenith angles in the tropics.

**All-sky imager.** A self-made all-sky imager provides a high-resolution digital photo from the sky above the site every minute. It was a project of the apprentices of the Max Planck Institute for Meteorology (MPI-M) workshop based on a prototype from John Kalisch, who at the time was working at the Institute for Sea Research in Kiel, Germany. It consists of a digital camera Canon PowerShot G9 with 12.1 megapixels and a fish-eye objective Raynox DCR-CF185PRO built into an outdoor housing.

**Meteorological instrumentation.** Continuous meteorological measurements are provided by a Vaisala WXT520 sensor that is mounted to a mast above one of the seatainers. The sensor provides measurements of wind speed and direction, rainfall, temperature, humidity, and barometric pressure at 10-s intervals. During the field studies, such as Cloud, Aerosol, Radiation and Turbulence in the Trade Wind Regime over Barbados (CARRIBA) and Next-Generation Aircraft Remote Sensing for Validation Studies (NARVAL), radiosondes are launched once or twice per day from the site and are launched irregularly throughout

the year for ongoing calibration of the remote sensing instrumentation.

**SUPPLEMENTARY INSTRUMENTS.** Four webcams, oriented southeast, northeast, northward, and westward, take visible images of the site every minute. In addition, the BCO includes an array of supplementary instruments, some of which are quite sophisticated but have been operational only temporarily. These are described below.

**Water vapor DIAL.** The MPI water vapor differential absorption lidar (DIAL; Ertel et al. 2005) was operated for five months during the period between November 2011 and May 2012. The DIAL transmits in the near infrared, at 820 nm, where appropriate water vapor absorption lines are located. Elastic backscatter at two wavelengths, one adjusted to the maximum absorption and another one to the wing of the absorption line, provides the information on air humidity. Working with elastic scattering makes the technique nearly insensitive to the sky background and allows daytime retrievals of humidity, which is not possible with the present Raman lidar system. The laser cavity design allows adjusting the sounding wavelengths to the different absorption lines, which are selected according to typical air humidity in the region of observations. Usability of DIAL in the vicinity of low clouds was found to be limited because of the nonlinearities in the receiving chain formed by a detector, amplifiers, and an analog-to-digital converter. Different errors in signal gradients at online and offline wavelength require manual selection of trustworthy water vapor in the range of clouds. The DIAL was also of limited use for detecting humidity above the cloud layer due to insufficient backscattered energy.

**TABLE ES2. Uptime (percentage by season) of main BCO instrumentation in first 5 years of operation. MRR refers to the Metek Micro Rain Radar, two of which are operational: one at the CIMH and the other at the BCO. Seasons are as follows: Dec–Feb (DJF), Mar–Apr (MAM), Jun–Aug (JJA), and Sep–Nov (SON).**

	Season			
	DJF	MAM	JJA	SON
Cloud radar	59	38	55	46
Raman lidar	77	55	42	69
MRR-BCO	94	98	90	94
MRR-CMHI	84	99	99	73
Ceilometer	91	94	90	94
Cloud Camera	96	98	69	71
Weather	90	79	53	60

According to the DIAL data, the deviation of absolute humidity from the daily average value remains in the range of  $\pm 0.3 \text{ g m}^{-3}$ . So if a diurnal cycle is present, it is small. This gives us confidence that the nighttime humidities derived from the Raman system are representative of the daily average. The development of the new, high-powered system, which is capable of daytime humidity measurements will, however, let us test this supposition.

**Scanning precipitation radar.** The Barbados Meteorological Services maintains a high-performance METEOR 500S Gematronik radar. The radar operates in the S band (10 cm), is linearly (horizontal) polarized, and has been operational since 2008 with data archived since 2009. The radar uses two pulse lengths; the shorter 0.82-ms pulse provides a higher-range resolution of 125 m, a sensitivity of  $-4.7 \text{ dBZ}$  at 50 km, and an unambiguous range of 125 km. The longer 2-ms pulse yields a 300-m range resolution, a sensitivity of  $-12.5 \text{ dBZ}$  at 50 km, and an unambiguous range of 500 km. The antenna has an 8.5-m diameter, resulting in a beamwidth of  $1^\circ$ . A full  $360^\circ$  scan can be performed in 10 s. The scan strategy presently consists of five  $360^\circ$ -azimuth scans in 3 min, repeated every 5 min, so that there is a 2-min interval when no data are being collected. The five elevation angles used are  $0.0^\circ$ ,  $0.5^\circ$ ,  $2.2^\circ$ ,  $5^\circ$ , and  $15^\circ$ . The scanning strategy has evolved over time, but a 400-km surveillance scan at a low elevation angle has been performed every 15 min since the beginning of operations.

**Microwave radiometer.** The University of Cologne has been maintaining a scanning RPG Radiometer Physics GmbH Humidity and Temperature Profiler (HATPRO) radiometer (SUNHAT). SUNHAT has two receivers and measures seven brightness temperatures around the water vapor line at 22.24 GHz with  $3.3^\circ$ – $3.7^\circ$  resolution

and seven in the oxygen complex band at 60 GHz with  $2.2^\circ$ – $2.5^\circ$  resolution. The brightness temperatures from the water vapor line are used for water vapor profiling; the oxygen band measurements are used for temperature profiling. Measurements around the water vapor line are used to derive integrated water vapor (IWV) and integrated liquid water path (LWP) content. The instrument scans both in elevation and in azimuth with a step in the pointing angle from  $0.6^\circ$  to  $0.1^\circ$  in each direction. The SUNHAT provided data for most of 2011; it was removed for maintenance and has since been reinstalled and has been operating continuously since late 2013.

**Composition measurements at Ragged Point.** The University of Miami Rosenstiel School of Marine and Atmospheric Science maintains a site with two cargo container laboratories and a 17-m tower atop a 30-m cliff on Ragged Point, Barbados. Daily aerosol filter samples are collected atop the tower, and dust, non-sea salt sulfate, nitrate, and sea salt are measured. Dust burdens are highly variable but can be as high as  $200 \mu\text{g m}^{-3}$  during dust events, but even during the dustiest months concentrations are typically much lower with median values similar to sea salt burdens, which average around  $20 \mu\text{g m}^{-3}$  with only light seasonality (Fig. 8b). Burdens of nitrate and non-sea salt sulfate are much smaller. For the 10-yr period between 2000 and 2010, daily nitrate concentrations averaged  $0.49 \mu\text{g m}^{-3}$  with an interquartile range between  $0.30$  and  $0.79 \mu\text{g m}^{-3}$ . Daily sulfate concentrates averaged  $1.9 \mu\text{g m}^{-3}$  with an interquartile range between  $1.4$  and  $2.5 \mu\text{g m}^{-3}$ .

**NARVAL.** The NARVAL field study composed two major phases (Klepp et al. 2014). The South Phase was flown over the tropical and subtropical Atlantic in December 2013, and a North Phase examined precipitation from

**TABLE ES3. Overview of NARVAL South Phase flights. OBF is the airport code for Oberpfaffenhofen in southern Germany, and BGI stands for Grantley Adams International Airport in Barbados. All times are UTC.**

Mission	Date	Takeoff	A-Train	Landing	Comment
RF01	10 Dec 2013	1014 (OBF)	1507	2041 (BGI)	Transatlantic
RF02	11 Dec 2013	1429 (BGI)	1724	2158 (BGI)	Local flight
RF03	12 Dec 2013	1350 (BGI)	1629	2020 (BGI)	Mid-Atlantic
RF04	14 Dec 2013	1335 (BGI)	1629	2021 (BGI)	Mid-Atlantic
RF05	15 Dec 2013	1515 (BGI)	1700	2145 (BGI)	Mid-Atlantic, pitch and roll maneuvers
RF06	16 Dec 2013	1310 (BGI)	1605	2259 (OBF)	Transatlantic
RF07	10 Dec 2013	1005 (OBF)	—	1957 (BGI)	Transatlantic, coordinated operations with F20
RF08	10 Dec 2013	1620 (BGI)	1723	0235 (OBF)	Transatlantic

postfrontal systems in the storm tracks in January 2014. The South Phase was flown in support of operations at the BCO and is briefly summarized here.

Table ES3 lists important information from the eight NARVAL South Phase flights. Four of these flights crossed the Atlantic; the remainder took off and landed at Grantley Adams Airport. Three research flights (RF03–RF05) flew from Grantley Adams to the mid-Atlantic and returned along the same path, deviating only to fly a leg under the track of the A-Train at the time of its overpass. One research flight (RF02) flew a mattress-spring pattern east of Barbados encompassing an area of deep convection in the southern part of flight operations. One of the transatlantic legs (RF07) included 37 min of coordinated operations (1100–1137 UTC) with the French Falcon F20 sampling a convective system between Lyons and Tarbes, France. The Falcon operated its Radar System Airborne (RASTA) system that includes a W-band cloud radar and flew 2 km below High Altitude and Long Range Research Aircraft (HALO) at a flight level near 10 km.

Legs coinciding with an A-Train overpass varied in duration from 784 s for RF01 to 1,507 s for RF06, corresponding to leg lengths from 188 to 414 km. Clouds were fortuitously sampled on all A-Train overpass legs. An example is shown in Fig. ES1, which also shows that *CloudSat* provides a very good representation of the shallow convective systems observed over the central Atlantic, only missing features in the lowest 1 km of the atmosphere. When the Hurricane Aerosol and Microphysics Program (HAMP) measurements are degraded to the resolution of *CloudSat*, the match is even better. There is some indication that the W-band cloud radar aboard *CloudSat* is somewhat more sensitive to low clouds than is the Ka-band radar flown as part of HAMP. There is, however, also the indication that *CloudSat* misses some of the intense (>35 dBZ) but narrow precipitation features (e.g., the region of very strong returns in Fig. ES1).

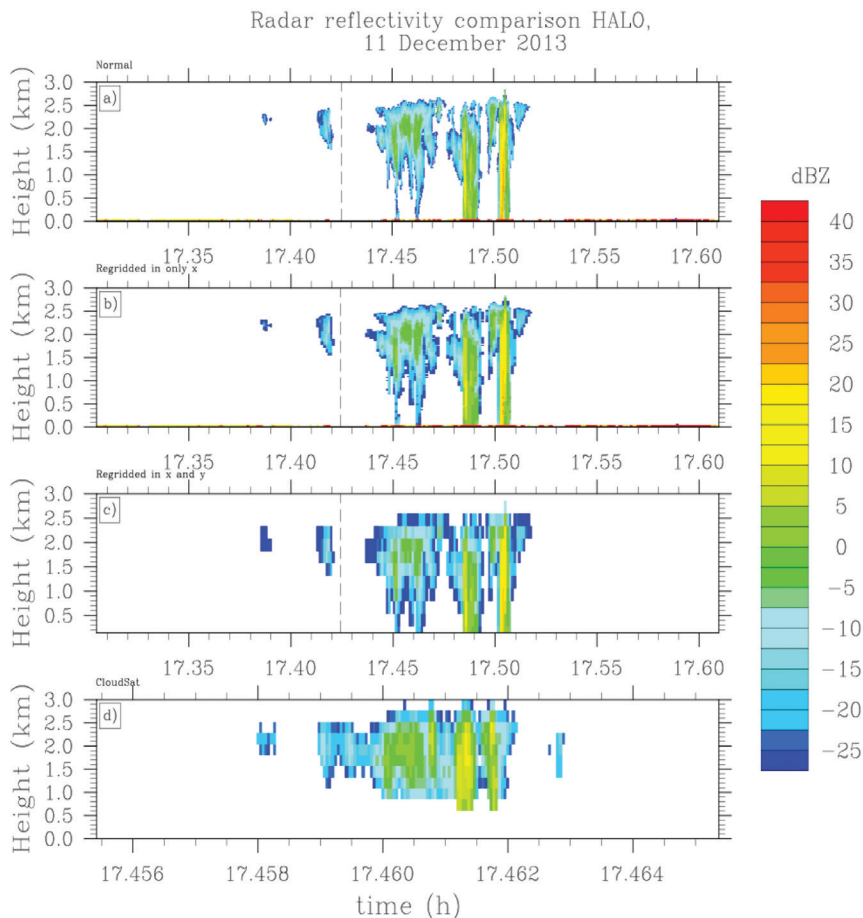


**FIG. ES1. *CloudSat* overpass along a HALO leg on 11 Dec 2013. Shown is the (a) Ka reflectivity from the HALO cloud radar, (b) regrided to match the resolution of *CloudSat* in the horizontal, (c) regrided to match *CloudSat* horizontal resolution and vertical range gating, and (d) *CloudSat* data. The point of coincidence is indicated by the dashed line.**

## REFERENCES

- Ertel, K., H. Linné, and J. Bösenberg, 2005: Injection-seeded pulsed Ti:sapphire laser with novel stabilization scheme and capability of dual-wavelength operation. *Appl. Opt.*, **44**, 5120–5126, doi:10.1364/AO.44.005120.
- Klepp, C., F. Ament, S. Bakan, L. Hirsch, and B. Stevens, 2014: NARVAL campaign report. Max Planck Institute for Meteorology Tech. Rep. 164, 218 pp. [Available online at [www.mpimet.mpg.de/fileadmin/publikationen/Reports/WEB\\_BzE\\_164\\_last.pdf](http://www.mpimet.mpg.de/fileadmin/publikationen/Reports/WEB_BzE_164_last.pdf).]
- Lonitz, K., B. Stevens, L. Nuijens, L. Hirsch, V. Sankt, and A. Seifert, 2015: The signature of aerosols and meteorology in long-term cloud radar observations of trade-wind cumuli. *J. Atmos. Sci.*, **72**, 4643–4659, doi:10.1175/JAS-D-14-0348.1.
- Nuijens, L., I. Serikov, L. Hirsch, K. Lonitz, and B. Stevens, 2014: The distribution and variability of low-level cloud in the North Atlantic trades. *Quart. J. Roy. Meteor. Soc.*, **140**, 2364–2374, doi:10.1002/qj.2307.